Colloid Polym Sci 275:486–492 (1997)


ORIGINAL CONTRIBUTION

L. Yang
N. Takisawa
T. Kaikawa
K. Shirahama

# Interaction of photosurfactants, 2-[4-(4-alkylphenylazo)phenoxy] ethyltrimethyl-ammonium bromides with γ-cyclodextrin and thermodynamics of complexation of photosurfactants with cyclodextrins

Received: 29 August 1996
Accepted: 13 November 1996

L. Yang · N. Takisawa · T. Kaikawa
Prof. K. Shirahama (✉)
Department of Chemistry
Faculty of Science and Engineering
Saga University
Saga 840, Japan

**Abstract** The stoichiometry, stability, and structure of the inclusion complex between the photosurfactants, 2-[4-(4-alkylphenylazo) phenoxy]ethyltrimethylammonium bromides (alkyl = ethyl, and butyl, where the abbreviations are EZ and BZ, and ZT for both, respectively), and γ-cyclodextrins (γ-CDx) in aqueous solution have been studied by the induced circular dichroism (ICD) and UV/VIS spectra as well as the potentiometric titration method. It is shown that the *trans*-ZT/γ-CDx systems form not only 1:1 (EZ) or 2:2 (BZ) but also 2:1 (ZT:γ-CDx) inclusion complexes. On the contrary, the steric hindrance of *cis*-ZT destabilizes the inclusion so that there is only 1:1 complex formation with γ-CDx. The thermodynamic discussion suggests that the stability of ZT complex is governed by the hydrophobic and the van der Waals interaction between the photosurfactants and cyclodextrins. However, the van der Waals interaction is more predominant in the *trans*-ZT/α-CDx system than in the β- and γ-CDx's except for $(BZ/\gamma\text{-CDx})_2$ system. Moreover, the alkylchain-length dependence of the free energy changes of complex formation of ZT and CDx are less than those of micellization of ZT because the cavity depth of CDx is limited to incorporate all hydrophobic parts of ZT. Finally, the isoequibrium temperature is estimated by the compensation plot of thermodynamic parameters.

**Key words** Photosurfactant – *trans/cis*-isomerization – cyclodextrin – complexation constant – enthalpy/entropy compensation – surfactant-selective electrode – induced circular dichroism

## Introduction

Azo compounds showing the photoinduced *trans–cis* isomerization are intriguing and widely studied as a synthetic photoresponsive model which can be subject to photoregulation [1]. On the other hand, cyclodextrins (CDx) have attracted great attention because of their ability to bind hydrophobic substrates into their cavities followed by physicochemical changes in aqueous solution. So it is a subtle strategy to combine these two systems into one. Actually there have been reported works such as photochemical reactions in the Langmuir–Blodgett (LB) films [2, 3], liposomes [4], photosensitive capped CDx [5–8], photoregulation of catalytic activity of β-CDx by azo inhibitor [9]. Also there are several thermodynamic and kinetic research on the complexation between azo compounds and CDx aqueous solution [10–14], and a crystal structure analysis of α-CDx–methyl orange complex [15]. Recently, there have been some works focusing on micellization [16, 17].

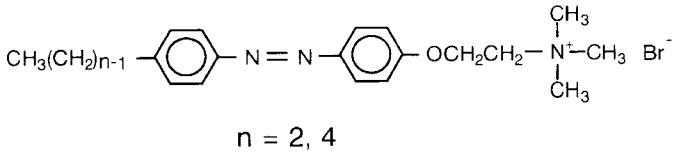


**Fig. 1** The chemical structure of ZT

We also investigated [18] the inclusion complex formation of photosurfactants, 2-[4-(4-alkyl phenylazo)phenoxy]ethyltrimethylammonium bromides (alkyl = ethyl, and butyl, where the abbreviations are EZ and BZ, and ZT for both, respectively) (Fig. 1) with α- and β-cyclodextrin (α-CDx, β-CDx, and CDx for both) in aqueous solutions by means of the induced circular dichroism (ICD) and UV/VIS spectra as well as the potentiometric titration (emf) method using a surfactant-selective electrode. The stoichiometry, formation constants, and the structures of inclusion complexes have been discussed in the paper which was preceded by our own paper describing more fundamental properties of the photosurfactant [17] where the micelle formation of *trans*- and *cis*-surfactants was discussed.

In the present paper, the complexation of ZT and γ-CDx is studied by the same ICD and emf methods following the previous paper [18]. The stoichiometry, formation constants, and the structure of the inclusion complexes are discussed. For the better and general understanding of the photosurfactant–CDx interaction, the results of α-, β-, and γ-CDx are shown in row and discussed from the viewpoint of thermodynamic and induced circular spectroscopy.

## Experimental section

### Materials

The photosurfactants ZT were prepared by azocoupling of *p*-alkylaniline with phenol, followed by alkylation with dibromoethane and quaternization with trimethylamine [16]. The γ-CDx was a commercial product (Wako Pure Chemical Ind. Co.) and used without further purification. Thermogravimetric analysis indicated that the γ-CDx used contains 8.5% (w/w) water.

### Equipments and procedures

The UV/VIS absorption and the circular dichroism were measured in a 10 mm quartz cell by a JASCO Ubest-30 UV/VIS spectrophotometer and a JASCO J720 spectropolarimeter, respectively. All the experimental conditions are the same as those described in Ref. [19]. The potentiometric measurements were carried out by using the same equipment as before [20].

## Results and discussion

### Stoichiometry and formation constant of inclusion complexes

The complexation constants between ZT and γ-CDx were determined by using an emf titration method. Typical potentiometric data of BZ are shown in Fig. 2 where two curves, one with γ-CDx, another without γ-CDx are displayed. The outline of the potentiometric data for the system with γ-CDx looks a little different from the one of β-CDx [18] in which the curve with γ-CDx deviates more from the calibration line at low ZT concentration rather than at high concentration of ZT. Furthermore, from the Scatchard plots for the binding of EZ and BZ to γ-CDx shown in Fig. 3, it seems that γ-CDx and ZT may form a 2:1 complex. So, we assume a 2:1 complex formation with γ-CDx.

$$S + CDx \overset{K_1}{\rightleftharpoons} S \cdot CDx \,, \tag{1}$$

$$S \cdot CDx + S \overset{K_{21}}{\rightleftharpoons} S_2 \cdot CDx \,. \tag{2}$$

Then the complexation constants $K_1$ and $K_{21}$ can be expressed as follows:

$$K_1 = [S \cdot CDx]/[S][CDx] \,, \tag{3}$$

$$K_{21} = [S_2 \cdot CDx]/[S][S \cdot CDx] \,, \tag{4}$$

with mass balance

$$[S]_0 = [S] + [S \cdot CDx] + 2[S_2 \cdot CDx] \tag{5}$$

$$[CDx]_0 = [CDx] + [S \cdot CDx] + [S_2 \cdot CDx] \tag{6}$$

where [CDx], $[CDx]_0$, [S], and $[S]_0$ are the equilibrium and total concentrations of CDx and ZT; [S · CDx] and [$S_2$ · CDx] the concentrations of 1:1 and 2:1 (S:CDx) complexes; $K_1$ the complexation constant of 1:1 (S:CDx), $K_{21}$ the complexation constant of 2:1 (S:CDx), respectively.

After combining Eqs. (3)–(6), we get

$$[S]_0 = [S] + [CDx]_0(K_1[S] + 2K_1K_{21}[S]^2) / (1 + K_1[S] + K_1K_{21}[S]^2) \,. \tag{7}$$

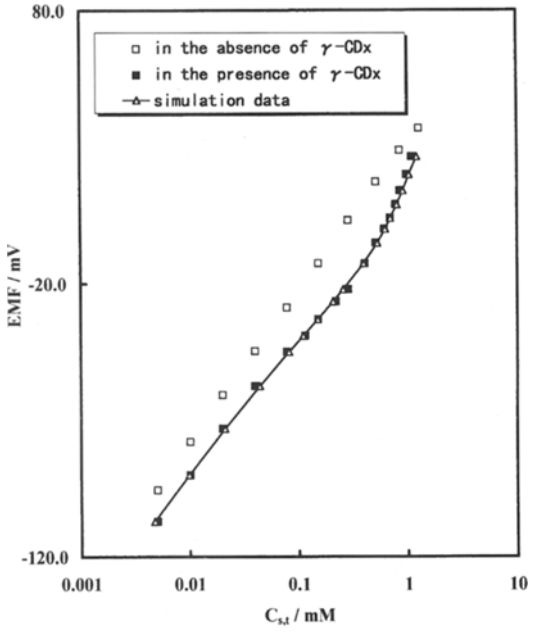


**Fig. 2** A typical potentiometric titration data of BZ with γ-CDx (0.5 mM) at 25 °C. $C_{s,t}$ is the total concentration of *trans*-BZ

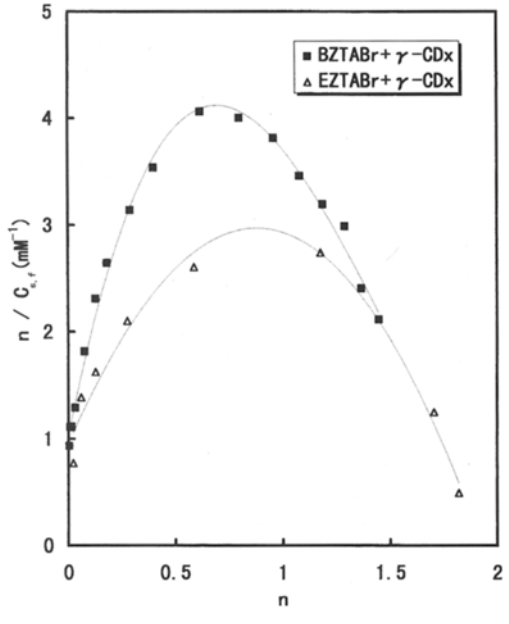


**Fig. 3** Scatchard plots for the binding of EZ and BZ to γ-CDx as obtained by the emf method at 25 °C. *n* is the average number of surfactant bound to a CDx molecule

A least-mean-square computer fitting program gives us $K_1$ and $K_{21}$ which fits Eq. (7) best to the experimental data and are presented in Table 1. A good curve fitting is seen in Fig. 2, where the solid line is the simulation result. It is

**Table 1** The complexation constants of the EZ/γ-CDx system

| | $T$ [K] | $K_1(K_{22})$ [$mM^{-1}$] | $K_{21}$ [$mM^{-1}$] |
|---|---|---|---|
| BZ | 298 | 1.20 | 16.3 |
| | 308 | 0.84 | 24.3 |
| | 318 | 0.24 | 40.2 |
| EZ | 298 | 0.41 | 21.4 |
| | 303 | 0.35 | 22.2 |
| | 308 | 0.36 | 23.3 |

*Note*: $K_{22}$ is only for BZ which will be mentioned in the text.

indicated that the binding of 1:1 complex decreases with increasing temperature, but that of 2:1 (S:CDx) has the opposite tendency to the 1:1 for EZ or 2:2 complexation for BZ (which will be mentioned later). Furthermore, the values of $K_{21}$ are much larger than those of $K_{22}$ (13–143 times for BZ and 50–64 times for EZ), which means that two ZT inclusion into the large cavity of γ-CDx makes a good size fitting and brings about a strong interaction between ZT and γ-CDx's inner wall.

## Spectral aspects of inclusion complex

### *UV/VIS spectra of ZT/γ-CDx*

The absorbance spectra are almost the same as the BZ/γ-CDx and EZ/γ-CDx systems, so only those for EZ/γ-CDx are shown in Fig. 4. In contrast to *trans*-ZT/α- and β-CDx [18], the spectra of *trans*-ZT shows a slight blue shift and absorbance decrease on adding γ-CDx, which may be caused by a 2:1 (S:CDx) complex formation.

### *ICD spectra of trans-ZT/γ-CDx*

The circular dichroism spectrum is expected to be induced at the absorption bands of achiral guest molecules, for example, azobenzene compounds, when they are included in the cavity of chiral CDx host molecule. This phenomenon is called induced circular dichroism (ICD) [21]. The ICD spectra of *trans*-EZ and BZ/γ-CDx are shown in Figs. 5A and B, respectively. The positive bands are seen around 370 and 430 nm for *trans*-EZ/γ-CDx, the band is little changed on adding γ-CDx and the intensity increases with increasing the concentration of γ-CDx. However, for *trans*-BZ/γ-CDx, while the position of positive band at 430 nm keeps unchanged on adding γ-CDx, the intensity is enhanced with increasing the concentration of γ-CDx till 2 mM, and then starts decreasing from 2 to 8 mM. Moreover, the position of positive band at ca. 370 nm gradually shifts to a short wavelength (from 370 to 345 nm at 0.2 and

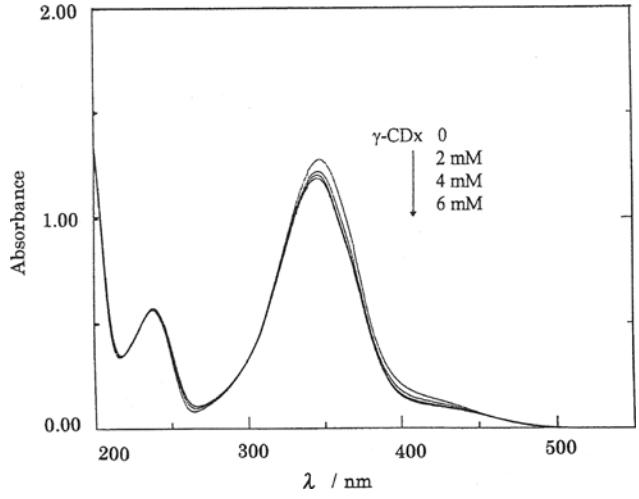


**Fig. 4** The absorbance spectra of EZ (0.05 mM) and γ-CDx (0, 2, 4, and 6 mM, at 25 °C)

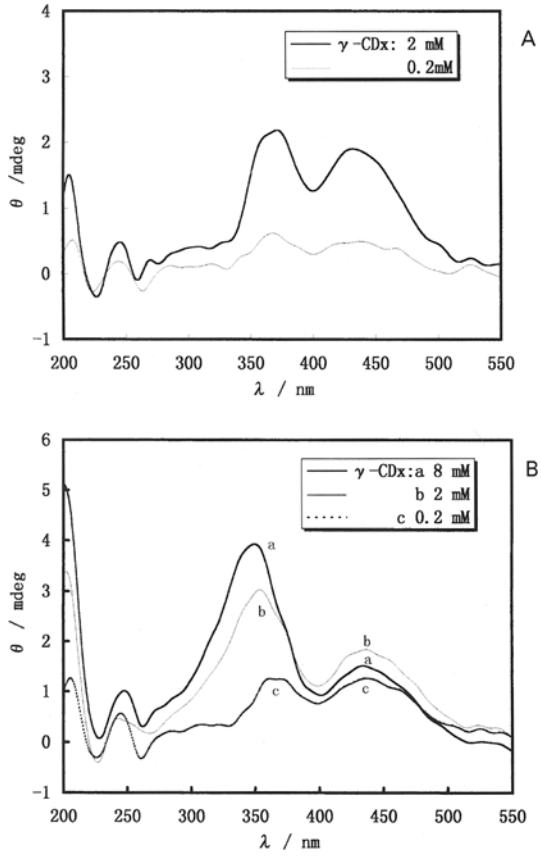


**Fig. 5** The ICD spectra of the inclusion complexes for **A** *trans*-ZT (0.05 mM) and **B** *trans*-BZ (0.05 mM) with γ-CDx at 25 °C

8 mM, respectively) on adding γ-CDx and the intensity increases with increasing γ-CDx concentration. Both ICD bands at ca. 370 and 430 nm correspond to the $\pi \rightarrow \pi^*$ and $n \rightarrow \pi^*$ transitions as observed in UV/VIS bands [18], respectively. It may be explained that the 2:1 (S:CDx) complex forms in the case of *trans*-EZ/γ-CDx system and *trans*-BZ at low γ-CDx's concentration (0.2 mM). There are two photosurfactant molecules in a γ-CDx cavity which shifts the $\pi \rightarrow \pi^*$ transition to a longer wavelength (370 nm) than α- and β-CDx system [18] where only one EZ molecule is accommodated. Even more increasing γ-CDx concentration, a 2:2 complex forms because of the longer alkyl chain of BZ, so that the $\pi \rightarrow \pi^*$ transition band gradually returns to about the same position as *trans*-ZT/α- and β-CDx's (ca. 350 nm).

### *ICD spectra of cis-ZT/γ-CDx*

Figure 6 shows the ICD spectra of *cis*-ZT/γ-CDx together with *cis*-EZ/β-CDx for comparison where the contents of *cis*-form are 93, 91, and 92% for β-CDx-EZ, γ-CDx-EZ, and γ-CDx-BZ systems, respectively, and sufficiently stationary for the time of experiment. It is noticed that a positive band around 430 nm and a negative band at ca. 310 nm of the γ-CDx system are very similar to the *cis*-EZ/β-CDx, which implies that *cis*-ZT forms 1:1 complex with γ-CDx. Even larger cavity of γ-CDx is too small to incorporate two bent-structured *cis*-ZTs.

### Thermodynamics of the interaction between ZT/CDx

It is noticed that the $K$ values decrease with increasing temperature as seen in Table 2. The van't Hoff plot (Eq. (8)) in which log $K$ is plotted against $1000/T$ gives an estimate of the enthalpy ($\Delta H^\circ$) as shown in Figs. 7A and B:

$$\log K = -\Delta H^\circ/(2.303RT) + C\,. \tag{8}$$

In addition, the free energy change ($\Delta G^\circ$) and $T\,\Delta S^\circ$ can be calculated, as

$$\Delta G^\circ = -RT \ln(55.5 \times K)\,, \tag{9}$$

$$-T\,\Delta S^\circ = \Delta G^\circ - \Delta H^\circ\,, \tag{10}$$

where the molarity of solvent water (55.5) is introduced to obtain a mole fraction-based free energy.

The standard free energy change ($\Delta G^\circ_m$) of micellization of ZT can be estimated from [22, 23]

$$\Delta G^\circ_m = (2 - q)RT \ln(\text{cmc}/55.5) \tag{11}$$

where $q$ is the degree of counterion binding. The thermodynamic parameters such as the standard free energy, enthalpy and entropy changes of the inclusion complexes of ZT and CDx, as well as the standard free energy of micellization are summarized in Table 2. It is seen in

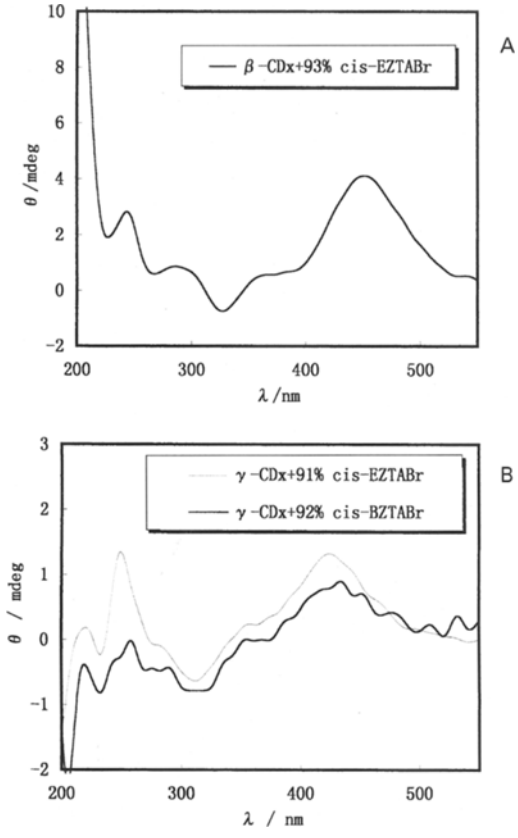


**Fig. 6** The ICD spectra of the inclusion complexes for *cis*-ZT at 25 °C. **A** between *cis*-EZ (0.05 mM) and β-CDx, and **B** between *cis*-ZT and γ-CDx, respectively. The concentration of CDx is 0.2 mM, and that of photosurfactant is 0.05 mM

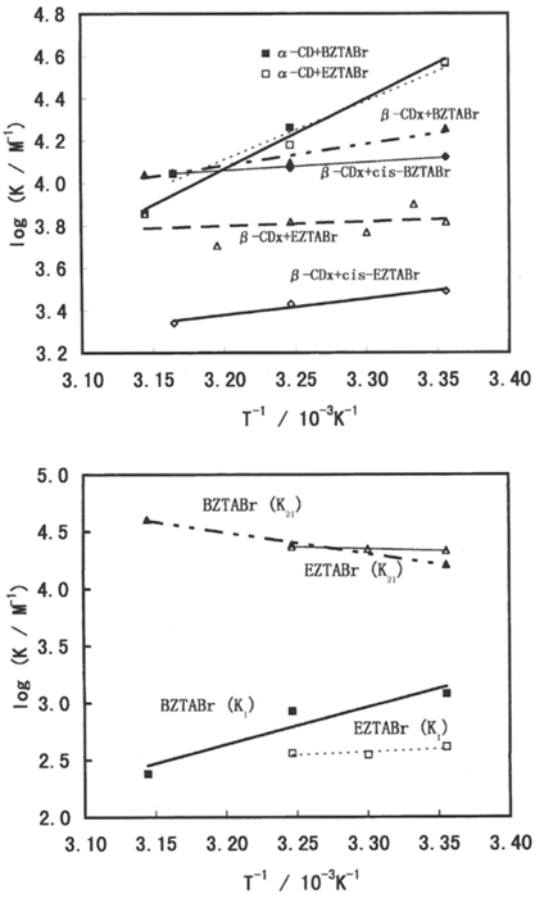


**Fig. 7** The van't Hoff plots of **A** ZT with β- and α-CDx, and **B** ZT with γ-CDx

Table 2 that *trans*-ZT forms a 1:1 inclusion complex with CDx whose affinity is in the order of α-CDx > β-CDx > γ-CDx: the tighter interaction between the smallest α-CDx cavity and the hydrophobic chain of photosurfactants leads to more favorable interaction, while the loose contact with larger CDx's to the decreased interaction, which can also be noticed in the enthalpy terms. The tighter interaction of α-CDx and ZT gives much more favorable enthalpy changes than β- and γ-CDx's. However, for the BZ/γ-CDx system, the enthalpy change is nearly as

**Table 2** The thermodynamic parameters of ZT inclusion compounds with CDx's at 25 °C

| | | | $\Delta G^\circ$ (kJ/mol) | $\Delta H^\circ$ (kJ/mol) | $-T\Delta S^\circ$ (kJ/mol) | $\Delta G_m^\circ$ (kJ/mol) |
|---|---|---|---|---|---|---|
| α-CDx | BZ | | −36.0[a)] | −73.2[a)] | 37.2[a)] | −43.6 |
| | EZ | | −36.0[b)] | −53.4[b)] | 17.4[b)] | −36.1 |
| β-CDx | BZ | | −34.2[a)] | −19.5[a)] | −14.7[a)] | −24.9 |
| | *cis*-BZ | | −33.5[b)] | −7.6[b)] | −25.9[b)] | −21.4 |
| | EZ | | −31.7[b)] | −3.7[b)] | −28.0[b)] | −36.1 |
| | *cis*-EZ | | −29.9[b)] | −15.3[b)] | −14.5[b)] | −16.0 |
| γ-CDx | $BZ/K_{22}$ | | −27.5[a)] | −63.0[a)] | 35.5[a)] | −43.6 |
| | | $K_{21}$ | −32.6[a)] | 35.5[a)] | −68.1[a)] | |
| | $EZ/K_1$ | | −24.9[a)] | −10.0[a)] | −14.9[a)] | −36.1 |
| | | $K_{21}$ | −34.6[a)] | 6.5[a)] | −41.1[a)] | |

[a)] EMF method.
[b)] ICD method.

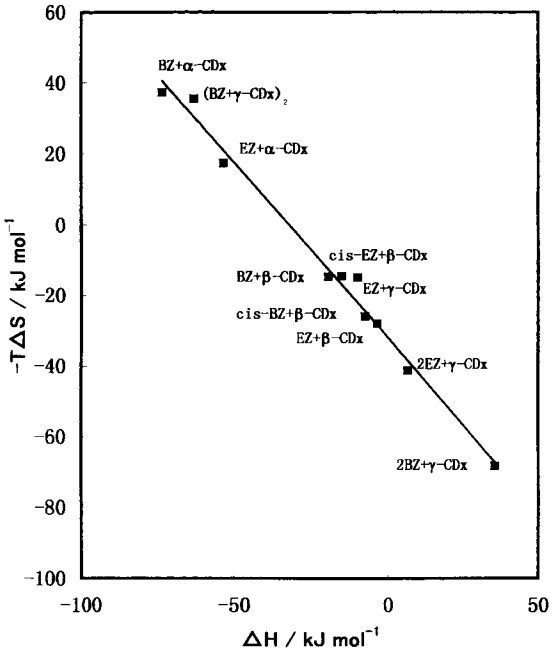


**Fig. 8** The compensation plot for the thermodynamic parameters of the complexation between ZT and α-, β- and γ-CDx

favorable as that of α-CDx's which suggests that BZ may form 2:2 complex with γ-CDx resulting from strong interaction between the cavity of γ-CDx and two BZ molecules. Therefore, it is reasonable to describe the complexation constant by $K_{22}$ for BZ instead of $K_1$. Furthermore, as alkyl chains of ZT increases, both the free energy changes of the complexation and micellization become more favorable. It suggests that the hydrophobic interaction is important in the complexation. However, there is no increase in the free energy change of complexation with increasing alkyl chains in the α-CDx systems. Because the relatively small cavity of α-CDx, in addition to the hydrophobic interaction, van der Waals force plays a more important role, in accordance with the above phenomena. It is also noticed that the difference of $\Delta G_m^\circ$ between the *trans*-BZ and *trans*-EZ is − 7.5 kJ/mol, while those of $\Delta G^\circ$ ranging from 0 to − 2.6 kJ/mol for α-, β- and γ-CDx are much smaller than the difference obtained from the dependence on alkylchain length for the micellization of ZT. It may be explained that the cavity depth of CDx is too much limited to completely incorporate the alkyl and azobenzene moieties of EZ. Moreover, for the *cis*-ZT, the complexation with α-CDx might be too small to be observed because of the steric hindrance of the bent molecular shape. For the same reason, for β-CDx, the free energy changes of *cis*-ZT are less favorable than those of *trans*-ZT which is governed by both enthalpy and entropy terms. The temperature dependence of *cis*-ZT with γ-CDx will be our future work. All the processes of complexation are exothermic except for the case of 2:1 (ZT:γ-CDx).

Figure 8 shows the enthalpy–entropy compensation of the complexation between ZT and α-, β- and γ-CDx . It is amazing that all the experimental points fall on a single line with the intercept of − 31.8 kJ/mol where there is no contribution from entropy term ($-T\Delta S^\circ = 0$). In addition, the slope of straight line gives the isoequilibrium temperature of 295 K, implying that, the enthalpy is compensated by the entropy at this temperature. The theoretical consideration on the enthalpy–entropy compensation has been described in more detail recently by Horváth et al. [24].

## Conclusion

The study of complexation of photosurfactants (ZT) and γ-cyclodextrin (γ-CDx) indicates that *trans*-ZT forms 1:1 (EZ) and 2:2 (BZ) complexes as well as 2:1 (ZT:γ-CDx) because of a big size of γ-CDx cavity. The inclusion complex formation between *cis*-ZT and CDx is sterically hindered by the folded molecular structure of the *cis*-photosurfactants. The *cis*-ZT forms 1:1 complex with γ-CDx in much the same way as *cis*-ZT/β-CDx systems, because the cavity size of γ-CDx is not so big enough to incorporate two bent-structured *cis*-ZT. Finally, all the complexation are exothermic except for the 2:1 (*trans*-ZT:γ-CDx) complex.

**Acknowledgment** This work is partially supported by a Grant-in Aid (No. 06640749) from the Ministry of Education, Science and Culture of the Japanese Government. A financial support from President Takashi Itoh, Process Lab. Micron Co. to L. Yang is greatly appreciated. The authors also are grateful to Dr. H. Kodama and Dr. M. Jelokhani-Niaraki of Saga University for their experimental assistance in ICD measurements and Dr. Y. Eda and Mr. T. Eguchi of Saga University for their many helpful suggestions and discussion.

## References

1. Erlanger BF (1976) Ann Rev Biochem 45:267–283
2. Yabe A, Kawabata Y, Niino H, Matsumoto M, Ouchi A, Takahashi H, Tamura S, Tagaki W, Nakahara H, Fukuda K (1988) Thin Solid Films 160:33–41
3. Niino H, Yabe A, Ouchi A, Tanaka M, Kawabata Y, Tamura S, Miyasaka T, Tagaki W (1988) Chem Lett 1227–1230

Colloid & Polymer Science, Vol. 275, No. 5 (1997)



4. Moss RA, Jiang W (1995) Langmuir 11:4217–4221
5. Ueno A, Takahashi K, Osa T (1981) J Chem Soc Chem Comm 94–96
6. Ueno A, Saka RK, Osa T (1979) Chem Lett 841–844
7. Ueno A, Yoshimura H, Saka R, Osa T (1979) J Am Chem Soc 101:2779–2780
8. Fukushima M, Osa T, Ueno A (1991) Chem Lett 709–712
9. Ueno A, Takahashi K, Osa T (1980) J Chem Soc Chem Comm 837–838
10. Cramer F, Saenger W, Spatz HCh (1967) J Am Chem Soc 89:14–20
11. Yoshida N, Fujita Y (1995) J Phys Chem 99:3671–3677
12. Yoshida N, Seiyama A, Fujimoto M (1990) J Phys Chem 94:4246–4253
13. Yoshida N, Seiyama A, Fujimoto M (1990) J Phys Chem 94:4254–4259
14. Harada A, Takahashi S (1987) J Chem Soc Chem Comm 527–528
15. Harata K (1976) Bull Chem Soc Jpn 49:1493–1501
16. Hayashita T, Kurosawa T, Miyata T, Tanako K, Igawa M (1994) Colloid Polym Sci 272:1611–1619
17. Yang L, Takisawa N, Hayashita T, Shirahama K (1995) J Phys Chem 99:8799–8803
18. Yang L, Takisawa N, Kaikawa T, Shirahama K (1996) Langmuir 12: 1154–1158
19. Takisawa N, Hall DG, Wyn-Jones E, Brown P (1988) J Chem Soc Faraday Trans 1, 84:3059–3070
20. Shirahama K, Watanabe T, Harada M (1988) In: Bloor DM, Wyn-Jones E (eds) The Structure, Dynamics and Equilibrium Properties of Colloidal Systems. Kluwer Academic Publishers, Netherlands, pp 161–172
21. Steiner RF, Garone L (1991) The Physical Chemistry of Biopolymer Solutions: Application of Physical Techniques to the Study of Proteins and Nucleic Acids. World Scientific, London, pp 220–237
22. Takisawa N, Shirahama K, Tanaka I (1993) Colloid Polym Sci 271:499–506
23. Moroi Y, Matuura R (1988) Bull Chem Soc Jpn 61:333–339
24. Vailaya A, Horváth C (1996) J Phys Chem 100:2447–2455